

Acidic C–H Bond as a Proton Donor in Excited State Intramolecular Proton Transfer Reactions

Anton J. Stasyuk,^{†,‡} Michał K. Cyrański,^{*,‡} Daniel T. Gryko,^{*,†,§} and Miquel Solà^{*,||}

[†]Faculty of Chemistry, Warsaw University of Technology, Noakowskiego 3, 00-664 Warsaw, Poland

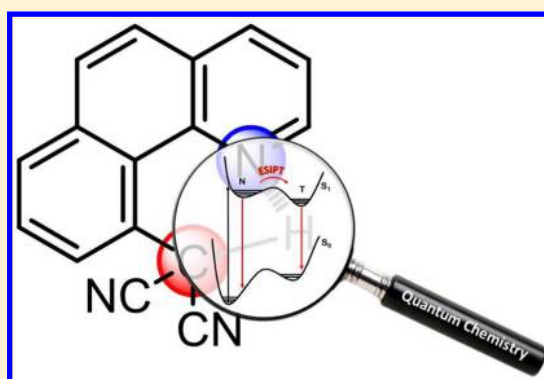
[‡]Department of Chemistry, University of Warsaw, Pasteura 1, 02-093 Warsaw, Poland

[§]Institute of Organic Chemistry of the Polish Academy of Sciences, Kasprzaka 44/52, 01-224 Warsaw, Poland

^{||}Institut de Química Computacional i Catàlisi and Departament de Química, Universitat de Girona, Campus Montilivi, 17071 Girona, Catalonia, Spain

S Supporting Information

ABSTRACT: An unprecedented type of excited state intramolecular proton transfer in a series of benzo[*h*]quinoline (BHQ) derivatives substituted at position 10 with strong CH acid character is described using density functional theory/time-dependent density functional theory computational approaches with a hybrid functional and the 6-311++G(d,p) triple- ξ quality basis set. Our results show that for 10-malononitrile-substituted BHQ (2CNBHQ) the excited state intramolecular proton transfer C–H...N reaction is a barrierless process. Calculations also reveal that the reaction profiles of the 4-amino-substituted 2CNBHQ show a large dependence on the polarity of the environment.



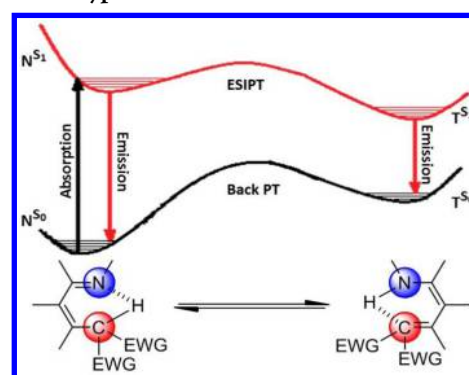
1. INTRODUCTION

Proton transfer is one of the most important and at the same time fundamental processes in chemistry, biology, and related fields. Proton transfer becomes increasingly important when it is associated with a photonic excitation.^{1–3} Numerous organic compounds possess both basic and acidic functional groups, whose properties may change (typically increase)^{4,5} during the transition from the ground state to the excited state. Generally, the proton transfer process from acidic group to proton acceptor occurs when a simultaneous change in the proton donor and proton acceptor properties is sufficiently significant. This process, known as an excited state intramolecular proton transfer (ESIPT),^{6,7} continues to be a subject of intensive scientific research even decades after the discovery of this phenomenon by Weller in 1955.^{8,9} Typically, ESIPT reaction is an extremely fast process occurring on the femto- to picosecond time scale. The ultrafast nature of ESIPT accompanied by a large Stokes shift provides numerous opportunities for the use of such compounds in a variety of applications, such as UV photostabilizers,^{10–13} filtered materials,¹⁴ fluorescent solar concentrators,^{15,16} laser dyes,^{17–19} fluorescent sensors,^{20–25} probes for biological environments,²⁶ organic light-emitting devices,^{27,28} etc.

It is generally accepted that the driving force of ESIPT reaction comes from significant changes in the acidity and basicity of the involved groups.^{29,30} In the ground state (S_0), the ESIPT molecules are mostly stable in the “normal” form (N^{S_0}). Excitation of this form by UV irradiation leads to the so-

called Franck–Condon S_1 excited state (N^{S_1}), which immediately undergoes a proton transfer to new tautomer S_1 , often called the “transferred” form (T^{S_1}) (Scheme 1).

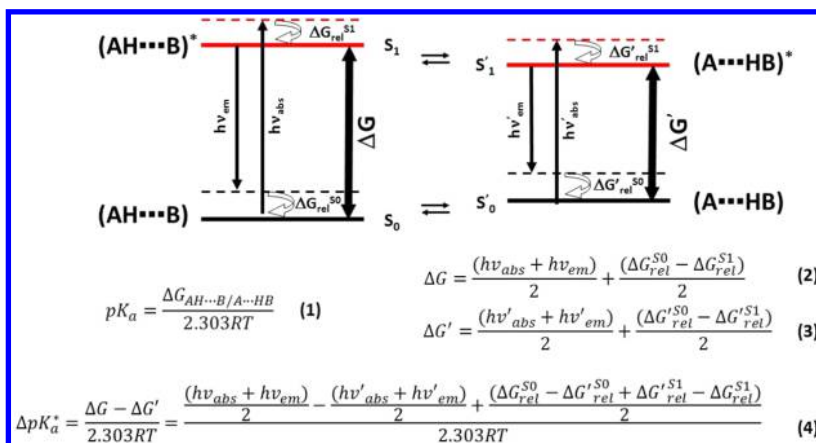
Scheme 1. A Typical ESIPT Process



ESIPT processes typically take place through the formation of a six-membered ring (five-membered^{31,32} or seven-membered^{33,34} units have also been described but are much rarer) with a strong intramolecular hydrogen bond between proton donor and acceptor groups. In the vast majority of described ESIPT-capable systems, phenolic -OH or -NH

Received: December 5, 2014

Published: February 3, 2015

Scheme 2. Energy Levels for the General Photoacid [(AH...B)*] and Its Conjugated Base [(A...HB)*] in Solution^a

^a S_1 and S'_1 are the excited states of the acid and base, respectively, S_0 and S'_0 are the ground states of the acid and base, respectively. $h\nu_{abs}$ and $h\nu_{em}$ are energies of absorption and emission transitions, respectively. The Förster energy gaps are the free energy gaps separating the thermodynamically relaxed ground state and the thermodynamically relaxed excited state energy levels of the photoacid (ΔG) and photobase ($\Delta G'$). $\Delta G_{rel}^{S_0}$ and $\Delta G_{rel}^{S_1}$ are the relaxation Gibbs energies of the acid immediately following the electronic transition in the ground and excited states, respectively. $\Delta G'_{rel}^{S_0}$ and $\Delta G'_{rel}^{S_1}$ are the same relaxation energies for the base.

groups serve as a proton donor group, whereas a heterocyclic nitrogen atom of the pyridine type or a carbonyl group acts as an acceptor of the proton.^{35–41} The first example of a “different” type of ESIPT from a phenolic –OH group to a carbon atom was discovered by Yates and co-workers^{42,43} during the study of photohydration reactions of *o*-hydroxystyrene. At the same time, these authors showed that the reverse proton transfer (from C–H to phenolate oxygen) is highly unfavorable. Later, Wan and co-workers^{44,45} significantly expanded the range of compounds with this type of ESIPT, showing the possibility of the excited state proton transfer from the phenolic group to a carbon atom that is part of an aromatic ring with a high quantum efficiency.^{46–48} This new type of ESIPT provides a new demonstration of the great importance of the acid–base chemistry of excited states. Taking into account the fact that even a base as weak as a carbon atom may act as an efficient proton acceptor under certain conditions, we wonder whether a proton directly connected to a carbon atom can participate in ESIPT.

Herein, we report the design and computational study of 10-substituted benzo[*h*]quinolines (BHQs) that constitute the first example of a fundamentally new type of ESIPT, the one corresponding to a proton transfer in the excited state from an acidic C–H center to a heterocyclic nitrogen atom.

2. COMPUTATIONAL DETAILS

Geometry optimizations were performed to explore minimum energy structures for ground state S_0 and first excited state S_1 using density functional theory (DFT) and time-dependent DFT (TDDFT) with the PBE1PBE⁴⁹ (hereafter also termed PBE0, its usual name in the literature) hybrid functional for the ground and first excited singlet states, respectively. This functional provides a good description of hydrogen bond interactions^{50,51} as well as of excited states.^{52,53} Here, the S_1 state has the $1(\pi\pi^*)$ -excited electronic configuration. Pople’s 6-311++G(d,p) triple- ξ quality basis set⁵⁴ with polarization and diffused functions was employed in both cases. Normal mode vibrational frequencies were also calculated in each case to confirm the presence of the local minimum, at the same level of theory. To simulate the effect of solvent, the geometries of

selected conformers were optimized using a self-consistent reaction field (SCRF) approach coupled with integral equation formalism of the polarizable continuum model (IEFPCM).^{55–57} All calculations were carried out using Gaussian 09.⁵⁸

Topological analyses of the electron distributions were conducted according to the “Quantum Theory of Atoms in Molecules” (QTAIM) proposed by Bader.^{59,60} The QTAIM calculations were performed using the AIMALL suite of programs⁶¹ to evaluate bond and ring critical point properties and the associated bond descriptors.

3. RESULTS AND DISCUSSION

Structural analysis of compounds with proton transfer in the excited state allows us to assert that the majority of ESIPT-capable systems can be classified as “flexible”; i.e., they can exist in several conformational states.^{62–64} In systems comprising only one potential proton donor and acceptor, the ESIPT is possible only in one “suitable” conformer, while the role of the others is the formation of additional deactivation channels. Furthermore, the polarity of environment may have a significant effect on the conformational equilibrium and, as a consequence, the proton transfer process. Taking into account this finding and the fact that the quantum efficiency of the process ESIPT is often relatively small,^{65,66} and in the case of weak acids and bases can be even smaller,⁶⁷ we decided to focus our attention on “rigid” (inflexible) systems with one main conformational state. Because the classical and most explored example of such rigid molecules is 10-hydroxybenzo[*h*]quinoline,^{68–70} we have chosen benzo[*h*]quinoline as a main core for our investigation.

3.1. Selection of Potential Candidates for Excited State Intramolecular CH Proton Transfer. Following the aim of our work, we have taken into consideration several structural fragments, which are in fact CH acids, and can potentially act as a donor of the proton. More often, the role of the proton donor is played by a hydroxyl group (usually linked to the aromatic moiety) because of its relatively high acidity. To date, there have been a sufficiently large number of known and well-studied CH acids. Some of them have acidity constant

values comparable with those of the most acidic phenols.^{71,72} However, it should be remembered that in the process of proton transfer in the excited state the key role belongs not to acidity and basicity but to photoacidity and photobasicity. Photoacids and photobases are organic dyes that become stronger acids and stronger bases (pH jump), respectively, in the electronic excited state. The most striking difference between the acidity and photoacidity can be represented by the Förster cycle (Scheme 2).

Thus, possible ESIPT compounds showing proton transfer from a carbon atom can be represented in the general form as a benzo[*h*]quinoline core, where the substituent at position 10 must be a strong CH acid (Figure 1). Needless to say, we have

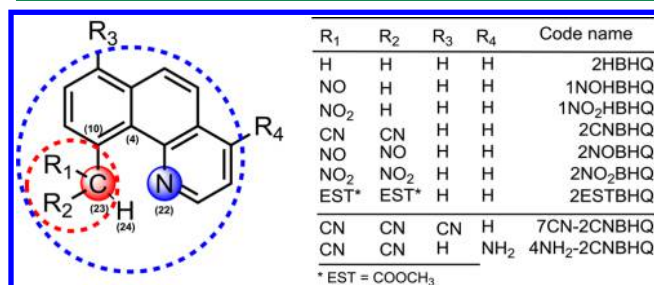


Figure 1. Different benzo[*h*]quinoline substituted derivatives and their code names.

several ways to influence the acidic and basic centers of the molecule, thereby allowing us to tune the propensity of the molecule for ESIPT. Formally, the whole process of the modeling of ESIPT-capable structures has been divided into two stages illustrated in Figure 1 by two circles. In the internal (red) circle, we can essentially increase the acidity of the proton by varying the substituents (R₁ and R₂) at the carbon atom directly connected with that proton. To achieve this goal, substituents R₁ and R₂ should exhibit pronounced electron-withdrawing properties. In the external (blue) circle, substituents R₃ and R₄ affect both the acidity of the proton donor center and the basicity of the core nitrogen atom acting as a proton acceptor. The electron donor properties of substituent R₄ have to increase the basicity of the nitrogen atom, while the electron-withdrawing character of substituent R₃ should increase the acidity on the proton. It is also worth remembering that electron-withdrawing properties of R₃ can also lower the basicity of the core nitrogen atom because of the resonance

effect. Clearly, in the case in which all substituents are protons, the ESIPT is out of the question, and this structure is used only as a reference point. Steps of the second circle were applied only to the most promising structure from the first group.

Despite the active study of the properties of CH acids over the past 50 years, information about their acidity is not available. Additionally, it should be noted that the calculation of the photoacidity from estimated values of Gibbs energies in ground and excited states requires a huge amount of computational resources, particularly for the calculation of the Gibbs energy in the excited state (eq 4, Scheme 2). We considered that because of the similarity of the structures as well as the electronic nature of the considered compounds, a symbiotic change in acidity and photoacidity could probably be expected. Although this hypothesis is obviously just a rough approximation, we decided to use it as a primary criterion for the selection of ESIPT-capable structures. However, even in this form, verification of all potential ESIPT compounds seems to be a quite time-consuming task. Taking into account the fact that a linear relationship exists between the acidity and the strength of the intramolecular hydrogen bond,^{73,74} we decided to switch from direct estimation of the acidity for each CH acid to the assessment of the strength of the C–H...N interaction.

The strength of the intramolecular hydrogen bond (C–H...N) can be estimated by different methods, including the classical approach based on homodesmotic reactions, NBO analysis, or topological analysis via the QTAIM approach. Given the relative inexpensiveness of the QTAIM calculations, we have chosen topological analysis as the primary selection criterion. Thus, the existence of a hydrogen bond was characterized by a QTAIM analysis of the topology of the electron density, $\rho(r)$. In particular, we analyzed the presence of a bond critical point (BCP, [3,–1] type) between the hydrogen atom and the acceptor atom, and we calculated $\rho(r)$ and the Laplacian of the electron density, $\nabla^2\rho(r)$, at the BCP.^{75,76} On the other hand, the hydrogen bond energy, E_{HB} , can be estimated from the potential energy density, $V(r)_{\text{BCP}}$. The strength of the H-bond is also related to the electron delocalization index between the proton acceptor and the transferred proton, $\text{DI}(\text{H}, \text{N})$.^{59,60,77}

To determine the lowest-energy conformer(s) in the series of 10-substituted benzo[*h*]quinolines of Figure 1, we conducted a systematic conformational analysis in the gas phase. The conformational space was analyzed by changing dihedral angle D_1 [C⁽⁴⁾–C⁽¹⁰⁾–C⁽²³⁾–H⁽²⁴⁾] that defines the relative position

Table 1. Selected Geometrical and Bond Critical Point Parameters Related to the Hydrogen Bonds for Studied Compounds in the Gas Phase

molecule/conformer	R , Å [N ⁽²²⁾ –H ⁽²⁴⁾]	dihedral angle D_1 , deg	$\rho(r)$, atomic units	$\nabla^2\rho(r)$, atomic units	$V(r)$, atomic units	DI, electrons [N ⁽²²⁾ –H ⁽²⁴⁾]
2HBHQ ^a	2.527	59.1	–	–	–	–
1NOHBHQ-sym	2.313	48.7	+0.0196	+0.0734	–0.0131	0.0526
1NOHBHQ-asy	2.197	38.9	+0.0223	+0.0791	–0.0146	0.0691
1NO ₂ HBHQ-sym ^a	2.453	61.5	–	–	–	–
1NO ₂ HBHQ-asy ^a	2.378	46.6	–	–	–	–
2CNBHQ	1.878	0.0	+0.0394	+0.1123	–0.0313	0.1249
2NOBHQ-syn	1.999	2.8	+0.0310	+0.1004	–0.0222	0.1022
2NOBHQ-anti	2.036	23.7	+0.0297	+0.0978	–0.0207	0.0940
2NO ₂ BHQ	2.227	39.6	+0.0233	+0.0859	–0.0164	0.0555
2ESTBHQ-syn	2.324	43.9	+0.0200	+0.0771	–0.0144	0.0487
2ESTBHQ-anti	2.302	40.6	+0.0203	+0.0774	–0.0144	0.0479

^aNo BCP was found for the H...N interaction.

Table 2. Vertical Excitation Properties Calculated for Selected Molecules with PBE0 and CAM-B3LYP Functionals

molecule/conformer	PBE0/6-311++g(d,p)			CAM-B3LYP/6-311++g(d,p)		
	$\pi\pi^*_{\text{min}}$, eV	$\lambda^{\text{calc}}_{\text{abs}}$, nm	f	$\pi\pi^*_{\text{min}}$, eV	$\lambda^{\text{calc}}_{\text{abs}}$, nm	f
2NOBHQ-syn	1.641	755.49	0.0013	1.618	766.40	0.0002
2NOBHQ-anti	1.650	751.62	0.0001	1.613	768.57	0.0000
2CNBHQ	3.994	310.39	0.0439	4.591	270.07	0.0378

of the benzo[*h*]quinoline core and the substituent(s). Substituents R_3 and R_4 considered in this work do not affect the total number of conformers because of the axial symmetry of these substituents. The dihedral angle was modified in 10° steps. For each dihedral angle, the geometry was reoptimized keeping constant the dihedral angle(s). Finally, the most stable conformers found were fully optimized, and the eigenvalues of their Hessians revealed that all structures described below correspond to minima.

We found that each monosubstituted structure can exist in two conformer forms with different values of dihedral angle D_1 (see Figure S1 of the Supporting Information). In the case in which R_1 and R_2 are distinct from H, for ester and nitroso substituents the existence of two conformers with different relative orientations of one substituent with respect to the other is possible (see Figure S2 of the Supporting Information). For each conformer found, hydrogen bond analysis, within the QTAIM framework, was conducted. Obtained results are listed in Table 1.

As expected, the performed topological analysis did not reveal the presence of a BCP in electron density $\rho(r)$ between $H^{(24)}$ and $N^{(22)}$ in 2HBHQ. This is the same situation found in the 10-methyl-substituted benzo[*h*]quinoline and also in the two conformers of 1-NO₂HBHQ. In all other cases studied, the topology of $\rho(r)$ confirms the presence of a BCP between $H^{(24)}$ and $N^{(22)}$. A more detailed analysis of this interaction was conducted through quantitative estimation of the electron density and its Laplacian $\nabla^2\rho(r)$. Good correlations were found between the $N^{(22)}-H^{(24)}$ bond length and $\rho(r)$ and $\nabla^2\rho(r)$ at the BCP, $DI[N^{(22)}-H^{(24)}]$, and hydrogen bond energies estimated on the basis of Espinosa's equation⁷⁸ as shown in Figure S3 of the Supporting Information. Additionally, kinetic energy density $[G(r)]$ and total electron energy density $[H(r)]$ at the BCP are also included in Table S1 of the Supporting Information. It is worth noting that the only species showing negative $H(r)$ values at BCP (indicative of a more covalent interaction) is 2CNBHQ.

All conformers showing a BCP in the hydrogen bond interaction were divided into three groups according to the strength of the hydrogen bond: (i) "strong", where $\rho(r) \geq 0.03$; (ii) "weak", where $\rho(r) \leq 0.02$; and (iii) "medium", where $0.02 \leq \rho(r) \leq 0.03$. In future work, we use only structures belonging to the "strong" group.

To gain insight into the possible occurrence of ESIPT, in the first stage we have conducted TDDFT PBE0/6-311++g(d,p) calculations of the vertical excitation properties. The results of the calculations determined that in the case of nitroso derivatives 2NOBHQ (both syn and anti conformers) the lowest-lying transition could correspond to a charge transfer process because of the low excitation energy and almost zero oscillator strength (f) (Table 2).

Taking into account the fact that the observed transitions may be an artifact associated only with the functional, as well as the fact that the non-Coulomb part of hybrid functionals typically dies off too rapidly and becomes very inaccurate at

large distances, making them unsuitable for some tasks associated with electron excitation modeling processes, we decided to repeat the calculations with the range-separated hybrid functional CAM-B3LYP.⁷⁹ Analysis of this transition shows that in this process several molecular orbitals are involved, but the main orbital (estimated by coefficients of the wave function for each excitation) is the HOMO–LUMO transition.

The electron density distribution confirms the presence of a charge transfer process for nitroso derivatives of benzo[*h*]quinoline (Figure 2). With this in mind, we decided to cease further consideration of nitroso-substituted systems and focus on the study of the 2CNBHQ molecule.

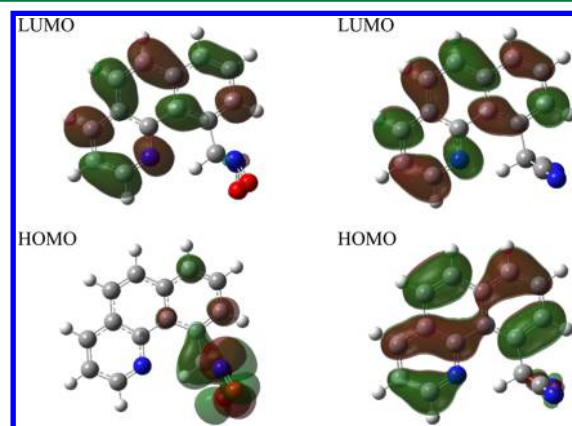


Figure 2. Kohn–Sham orbital representations for the HOMO and LUMO of 2NOBHQ-syn (left) and 2CNBHQ (right) obtained at the PBE0/6-311++g(d,p) level of theory.

3.2. The ESIPT Process in 2-(Benzo[*h*]quinolin-10-yl)malononitrile and Its Derivatives. The investigation of 2CNBHQ revealed that the proton-transferred form is stable in the ground state but does not correspond to a minimum in the S_1 potential energy surface (PES), thereby eliminating the ESIPT process. However, detailed analysis of the ground state tautomers ("pyridine" and "pyridinium") of 10-malononitrile-substituted benzo[*h*]quinoline showed that the dipole moment of the "pyridinium" form (11.24 D) is significantly larger than that for the "pyridine" form (7.98 D). Additionally, it has been found that the ground state and local excited state for "pyridine" are not particularly geometrically different, and as a result, their dipole moments are also close to each other (7.98 D for the ground state and 8.08 D for the local excited state). Given the larger dipole moment of the "pyridinium" form, we decided to repeat the calculations in a polar medium (ethanol; $\epsilon = 24.852$). In this case, the mutual stabilization of both "pyridinium" and "pyridine" forms was observed. Moreover, the "pyridinium" form in a polar solvent became a minimum on the S_1 PES. Summary data, including transition energies and oscillator strengths, are listed in Table S2 of the Supporting Information.

= 24.852). Analysis of the QTAIM data revealed a direct dependence of the hydrogen bond strength on the polarity of the environment within the IEFPCM model (Figure S4 of the Supporting Information). To verify the reliability and validity of the applied solvation model, we have also tested the conductor-like screening model as a variant of the continuum solvation model that uses a scaled conductor boundary conduction, and it is implemented in Gaussian 09 (CPCM).^{81–83} Both applied models provide essentially the same result (Table S3 of the Supporting Information). Figure 3 demonstrates the relative

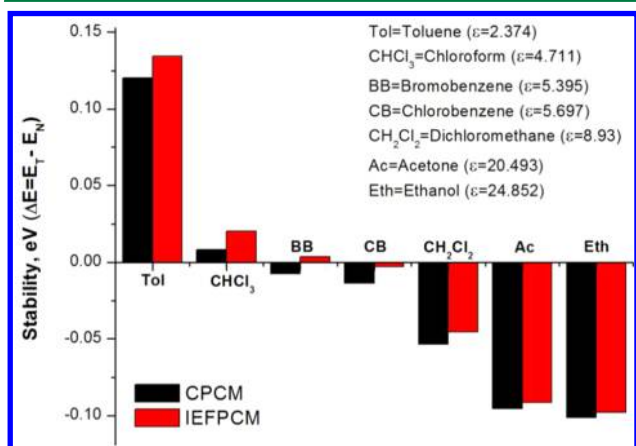


Figure 3. Relative stability of the ground state “pyridine” and “pyridinium” tautomers for 4NH₂-2CNBHQ in various solvents estimated within IEFPCM and CPCM solvation models.

stability of the “pyridinium” form (T^{S_0}) with respect to the “pyridine” form (N^{S_0}). Detailed data for the “pyridine” form of 4-amino-substituted 2CNBHQ in different environments are listed in Table S4 of the Supporting Information.

We found that the stability of 4NH₂-2CNBHQ tautomers is strongly dependent on the polarity of the environment. Interestingly, the change in solvent polarity can influence the composition of the equilibrium mixture of tautomers and consequently the fluorescence properties. Thus, in a less polar solvent, preferential stabilization of the less polar form (N^{S_0}) of 4NH₂-2CNBHQ is observed, while a more polar solvent largely stabilizes the more polar (T^{S_0}) form. On the basis of purely electrostatic solute–solvent interaction, the observed relative stabilities of the N^{S_0} and T^{S_0} forms correlate with the derivative of the Kirkwood function (Kirkwood equation),^{84–86} which relates the standard molar Gibbs energy of transfer molecules from the gas phase to a continuous medium of relative permittivity (ϵ), as well as with application of this equation for keto–enol equilibria, derived by Powling and Bernstein.⁸⁷ To verify the possibility of the ESIPT and to compare the behavior of 4-amino-substituted 2CNBHQ in various solvents, excited state calculations were performed (see Scheme 4).

Moving from a more polar solvent to a less polar solvent, we can manage the energy profile of 4NH₂-2CNBHQ to reach a profile similar to the typical energy profile of an ESIPT process. It is worth noting that the calculations were conducted in a PCM chloroform solution, despite the greater stabilizing effect of toluene as a solvent for the “pyridine” form in the ground state. The use of toluene as the solvent did not stabilize the “pyridinium” form of 4NH₂-2CNBHQ in the first excited state, and for this reason, this solvent was not considered in our calculations. The foregoing greater energy barrier for the proton transfer reaction in the excited state (6.25 kcal/mol, vs

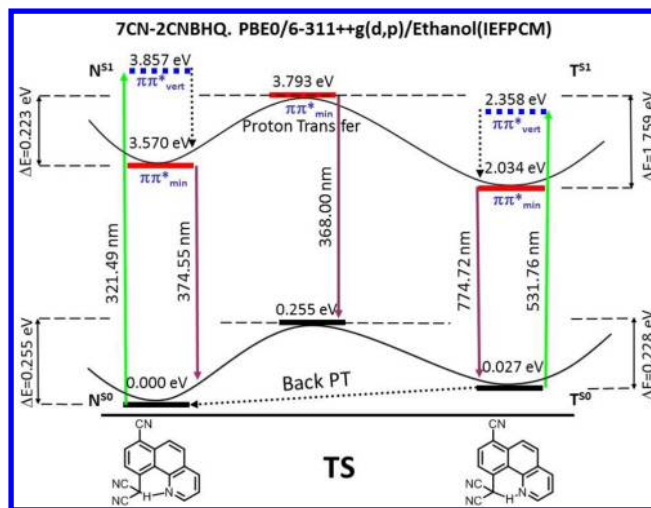
4.54 kcal/mol for the ground state in chloroform) allows us to assume a very low efficiency of the ESIPT in comparison with that of ground state proton transfer. Detailed data, including transition energies and oscillator strengths for 4NH₂-2CNBHQ in both ethanol and chloroform PCM solutions, are listed in Table S2 of the Supporting Information.

In the last stage of our work, we have studied 7-cyano-substituted 2CNBHQ by the same methodology that was used for previous molecules. As for 4NH₂-2CNBHQ, the QTAIM analysis of 7CN-2CNBHQ performed in the ground state indicates a slight increase in the acidity of the proton in the malononitrile group, which is also accompanied by a small increase in the $C^{(23)}-H^{(24)}$ bond length.

Surprisingly, in spite of the rather strong electron-withdrawing properties of the cyano group, as well as its “correct” location in the ring (para position with respect to the malononitrile fragment), the effect of this group in position 7 is negligible. This fact can probably be explained on the basis of the general idea of the negative mesomeric (M_-) effect of the cyano group. On one hand, the withdrawal of electron density promoted by the cyano group in a system with conjugated double bonds (benzo[*h*]quinoline core) causes some increase in the charge on the central carbon atom of malononitrile group and, as a consequence, leads to a small increase in the positive charge (increased acidity) on the transferred hydrogen atom. On the other hand, because of the mesomeric effect and its ability to act over long distances, the withdrawal of electron density from the nitrogen atom of the benzo[*h*]quinoline core to the substituent was also observed. This leads to a reduction of its basicity and, as a result, to a weakening of considered hydrogen bond strengths. Selected charge density data for 7CN-2CNBHQ and other considered molecules are listed in Table S5 of the Supporting Information.

Scheme 5 shows the results of a detailed investigation of the photochemical transformation of considered 7CN-2CNBHQ.

Scheme 5. Detailed Jablonski Diagram for the Singlet Excited State of 7CN-2CNBHQ in Ethanol



For this case, calculations revealed that the ESIPT is energetically favorable from a thermodynamic point of view. However, the activation energy of the transfer in the first excited state (5.14 kcal/mol) is only slightly lower than in the ground state (5.88 kcal/mol). Detailed data, including transition energies and oscillator strengths for 4CN-

Table 4. Bond Lengths and QTAIM Data in the Ground and Excited States for Studied Molecules

molecule	$C^{(23)}-H^{(24)}$				$H^{(24)}-N^{(22)}$			
	R, Å (C–H)	$\rho(r)$, atomic units	$\nabla^2\rho(r)$, atomic units	DI, electrons (C–H)	R, Å (N–H)	$\rho(r)$, atomic units	$\nabla^2\rho(r)$, atomic units	DI, electrons (N–H)
Ground State								
2CNBHQ ^a	1.113	0.2673	−0.9131	0.7286	1.826	0.0442	0.1145	0.1380
4NH ₂ -2CNBHQ ^a	1.121	0.2622	−0.8834	0.7055	1.773	0.0499	0.1169	0.1533
4NH ₂ -2CNBHQ ^b	1.117	0.2648	−0.8977	0.7162	1.791	0.0479	0.1171	0.1478
7CN-2CNBHQ ^a	1.113	0.2674	−0.9154	0.7259	1.817	0.0451	0.1159	0.1396
Excited State								
2CNBHQ ^a	1.124	0.2669	−0.9152	0.6940	1.770	0.0445	0.1125	0.1571
4NH ₂ -2CNBHQ ^a	1.102	0.2744	−0.9543	0.7552	1.908	0.0369	0.1080	0.1198
4NH ₂ -2CNBHQ ^b	1.106	0.2718	−0.9356	0.7477	1.870	0.0400	0.1132	0.1262
7CN-2CNBHQ ^a	1.105	0.2729	−0.9456	0.7519	1.889	0.0386	0.1112	0.1203

^aCalculation conducted for the IEFPCM/ethanol model. ^bCalculation conducted for the IEFPCM/chloroform model.

2CNBHQ in a PCM ethanol solution, are listed in Table S2 of the Supporting Information.

It is noteworthy that introduction of electron-donating or electron-withdrawing substituents in the corresponding positions of the benzo[*h*]quinoline ring leading to an increase in hydrogen bond strength does not lead to more effective ESIPT processes. On one hand, no perceptible increase in energy difference between “normal” and “transferred” forms of the ESIPT reaction was observed. The distinction for such an energy difference between 7-CN-substituted 2CNBHQ and unsubstituted 2CNBHQ is only 5.28 kcal/mol, while for the 4-amino derivative, the energy difference between tautomers of the ESIPT reaction is even smaller, with respect to parental 2CNBHQ by ~7.4 kcal/mol in chloroform and ~11.2 kcal/mol in ethanol. On the other hand, a significant increase in the activation energy for first excited state proton transfer has been observed. For 2CNBHQ, this transition is barrierless (0.6 kcal/mol), whereas for others, 4NH₂-2CNBHQ and 7CN-2CNBHQ, the activation energy is 10 times higher (6.25 and 6.64 kcal/mol for 4NH₂-2CNBHQ in chloroform and ethanol solutions, respectively, and 5.14 kcal/mol for 7CN-2CNBHQ in ethanol).

These results indicate the inapplicability of the selected criteria for the reliable description of driving force, namely changes in the acidity and basicity of the involved groups. However, the characteristics of the hydrogen bond estimated in the ground state are good selection criteria for the first stage of this work, the so-called first circle. The suitability of the selected criteria in one case and their utter uselessness in the other can be explained on the basis of electronic structure changes for the considered compounds depending on the position of the substituent. For compounds of the first circle, the applicability of all criteria is explained by their structural similarity and, as a result, the close trends of the electronic changes. In turn, for compounds of the second circle, a different position of the substituents with different electronic effects leads to an unsystematic unlocalized changes in the electronic structure. This obviously causes nonsymbatic changes in the acidity and photoacidity of considered compounds, whereas the symbatic change is the basic condition for the proper operation of selected criteria.

To verify this, we have performed a study of the hydrogen bond strength for all investigated compounds in their ground and first excited states (see Table 4).

QTAIM data strongly support the hypothesis that the changes in acidity and photoacidity occur inconsistently. Only in the case of unsubstituted 2CNBHQ does the transition to the first excited state lead to an increase in the acidity of the $C^{(23)}-H^{(24)}$ bond. This is supported by the increase in the $C^{(23)}-H^{(24)}$ bond length and corresponding changes in the BCP electron density and other QTAIM descriptors. In all other cases, the considerable reduction of the acidity of the $C^{(23)}-H^{(24)}$ bond and, as a result, the decrease in the hydrogen bond strength have been marked. For example, in the case of 4-amino-substituted 2CNBHQ in the first excited state, a 20% reduction in electron delocalization index $DI[N^{(22)}-H^{(24)}]$ was observed. In other cases, the decrease in this index was ~15%.

4. CONCLUSIONS

In conclusion, on the basis of TDDFT calculations, we have succeeded in demonstrating the existence of a novel and unique type of ESIPT. It has been proven that the acidity of the ArCH-RR' moiety can be sufficient to form a hydrogen bond in the ground state and to allow ESIPT to occur. For 4NH₂-2CNBHQ, we found an interesting feature, namely an extremely high sensitivity of the reaction profile to the polarity of the environment, affecting the tautomeric state of the molecule and consequently its fluorescence profile. These results not only are theoretically significant but also represent a conceptual breakthrough that allows the exploration of new horizons in the design of novel functional dyes.

■ ASSOCIATED CONTENT

Supporting Information

Cartesian coordinates for optimized ground and excited state geometries of all analyzed structures obtained using DFT/TDDFT with the PBE0 functional and Pople's 6-311++g(d,p) basis set, correlation between $N^{(22)}-H^{(24)}$ bond length and $\rho(r)$, $\nabla^2\rho(r)$, $DI[N^{(22)}-H^{(24)}]$, and hydrogen bond energy estimated via potential energy density $V(r)_{BCP}$, and the dependence of the hydrogen bond strength on the polarity of

the environment within the PCM model. This material is available free of charge via the Internet at <http://pubs.acs.org>.

AUTHOR INFORMATION

Corresponding Authors

*E-mail: chamis@chem.uw.edu.pl

*E-mail: dtgryko@icho.edu.pl

*Miquel Solà Institut de Química Computacional i Catàlisi and Departament de Química, Universitat de Girona, Campus Montilivi, 17071 Girona, Catalonia, Spain. E-mail: miquel.sola@udg.edu

Funding

A.J.S., M.K.C., and D.T.G. gratefully acknowledge the Foundation for Polish Science for supporting this work under Project MPD/2010/4 ("Towards Advanced Functional Materials and Novel Devices-Joint UW and WUT International PhD Programme"). This work has been also supported by the Ministerio de Economía y Competitividad (MINECO) of Spain (Project CTQ2011-23156/BQU) and the Generalitat de Catalunya (Project 2014SGR931, Xarxa de Referència en Química Teòrica i Computacional, and ICREA Academia 2014 prize for M.S.). A.J.S. gratefully acknowledges the European Social Fund through the Warsaw University of Technology Development Programme, realized by the Center for Advanced Studies.

Notes

The authors declare no competing financial interest.

REFERENCES

- (1) Agarwal, P. K.; Webb, S. P.; Hammes-Scheffer, S. *J. Am. Chem. Soc.* **2000**, *122*, 4803–4812.
- (2) Schowen, K. B.; Limbach, H.-H.; Denisov, G. S.; Schowen, R. L. *Biochim. Biophys. Acta* **2000**, *1458*, 43–62.
- (3) Chem, W.-H.; Xing, Y.; Pang, Y. *Org. Lett.* **2011**, *13*, 1362–1365.
- (4) Ireland, J. F.; Wyatt, P. A. H. *Adv. Phys. Org. Chem.* **1976**, *12*, 131–221.
- (5) Arnaut, L. G.; Formosinho, S. J. *J. Photochem. Photobiol., A* **1993**, *75*, 1–20.
- (6) Hsieh, C.-C.; Jiang, C.-M.; Chou, P.-T. *Acc. Chem. Res.* **2010**, *43*, 1364–1374.
- (7) Demchenko, A. P.; Tang, K.-C.; Chou, P.-T. *Chem. Soc. Rev.* **2013**, *42*, 1379–1408.
- (8) Weller, A. Z. *Electrochemistry* **1956**, *60*, 1144–1147.
- (9) Weller, A. Z. *Naturwissenschaften* **1955**, *42*, 175–176.
- (10) Parthenopoulos, D. A.; McMorro, D. P.; Kasha, M. *J. Phys. Chem.* **1991**, *95*, 2668–2674.
- (11) Catalan, J.; del Valle, J. C. *J. Am. Chem. Soc.* **1993**, *115*, 4321–4325.
- (12) Kaczmarek, L.; Borowicz, P.; Grabowska, A. *J. Photochem. Photobiol., A* **2001**, *138*, 159–166.
- (13) Sobolewski, A. L.; Domcke, W. *Phys. Chem. Chem. Phys.* **2006**, *8*, 3410–3417.
- (14) Lim, S.-J.; Seo, J.; Park, S. Y. *J. Am. Chem. Soc.* **2006**, *128*, 14542–14547.
- (15) Vollmer, F.; Rettig, W. *J. Photochem. Photobiol., A* **1996**, *95*, 143–155.
- (16) Mohammed, O. F.; Pines, D.; Nibbering, E. T. J.; Pines, E. *Angew. Chem., Int. Ed.* **2007**, *46*, 1458–1461.
- (17) Chou, P.-T.; McMorro, D.; Aartsma, T. J.; Kasha, M. *J. Phys. Chem.* **1984**, *88*, 4596–4599.
- (18) Chou, P.-T.; Martinez, M. L.; Clements, J. H. *Chem. Phys. Lett.* **1993**, *204*, 395–399.
- (19) Park, S.; Kwon, O.-H.; Kim, S.; Park, S.; Choi, M.-G.; Cha, M.; Park, S. Y.; Jang, D.-J. *J. Am. Chem. Soc.* **2005**, *127*, 10070–10074.
- (20) Kim, J. S.; Quang, D. T. *Chem. Rev.* **2007**, *107*, 3780–3799.
- (21) Wang, B.; Eric, V.; Anslyn, E. V. *Chemosensors: Principles, Strategies, and Applications*; Wiley: New York, 2011; pp 253–273.
- (22) Roshal, A. D.; Grigorovich, A. V.; Doroshenko, A. O.; Pivovarenko, V. G. *J. Phys. Chem. A* **1998**, *102*, S907–S914.
- (23) Svehkarev, D. A.; Karpushina, G. V.; Lukatskaya, L. L.; Doroshenko, A. O. *Cent. Eur. J. Chem.* **2008**, *6*, 443–449.
- (24) Liu, B.; Wang, H.; Wang, T.; Bao, Y.; Du, F.; Tian, J.; Li, Q.; Bai, R. *Chem. Commun.* **2012**, *48*, 2867–2869.
- (25) Zhao, J.; Ji, S.; Chen, Y.; Guo, H.; Yang, P. *Phys. Chem. Chem. Phys.* **2012**, *14*, 8803–8817.
- (26) Sytnik, A.; Kasha, M. *Proc. Natl. Acad. Sci. U.S.A.* **1994**, *91*, 8627–8630.
- (27) Park, S.; Kwon, J. E.; Kim, S.-H.; Seo, J.; Chung, K.; Park, S.-Y.; Jang, D.-J.; Medina, B. M.; Gierschner, J. Park, S.-Y. *J. Am. Chem. Soc.* **2009**, *131*, 14043–14049.
- (28) Kim, S.; Seo, J.; Jung, H. K.; Kim, J. J.; Park, S.-Y. *Adv. Mater. (Weinheim, Ger.)* **2005**, *17*, 2077–2082.
- (29) Barbara, P. F.; Walsh, P. K.; Brus, L. E. *J. Phys. Chem.* **1989**, *93*, 29–34.
- (30) Douhal, A.; Lahmani, F.; Zewail, A. H. *Chem. Phys.* **1996**, *207*, 477–498.
- (31) Bardez, E.; Devol, I.; Larrey, B.; Valeur, B. *J. Phys. Chem. B* **1997**, *101*, 7786–7793.
- (32) Zamotaiev, O. M.; Postupalenko, V. Y.; Shvadchak, V. V.; Pivovarenko, V. G.; Klymchenko, A. S.; Mély, Y. *Bioconjugate Chem.* **2011**, *22*, 101–107.
- (33) Chen, K.-Y.; Cheng, Y.-M.; Lai, C.-H.; Hsu, C.-C.; Ho, M.-L.; Lee, G.-H.; Chou, P.-T. *J. Am. Chem. Soc.* **2007**, *129*, 4534–4535.
- (34) Arai, T.; Moriyama, M.; Tokumaru, K. *J. Am. Chem. Soc.* **1994**, *116*, 3171–3172.
- (35) McMorro, D.; Kasha, M. *J. Phys. Chem.* **1984**, *88*, 2235–2243.
- (36) Shynkar, V. V.; Mély, Y.; Duportail, G.; Piémont, E.; Klymchenko, A. S.; Demchenko, A. P. *J. Phys. Chem. A* **2003**, *107*, 9522–9529.
- (37) Henary, M. M.; Wu, Y.; Cody, J.; Sumalekshmy, S.; Li, J.; Mandal, S.; J. Fahrni, C. J. *J. Org. Chem.* **2007**, *72*, 4784–4797.
- (38) Ciuciu, A. I.; Flamigni, L.; Skonieczny, K.; Gryko, D. T. *Phys. Chem. Chem. Phys.* **2013**, *15*, 16907–16916.
- (39) Forés, M.; Duran, M.; Solà, M.; Orozco, M.; Luque, F. J. *J. Phys. Chem. A* **1999**, *103*, 4525–4532.
- (40) Forés, M.; Duran, M.; Solà, M.; Adamowicz, L. *J. Phys. Chem. A* **1999**, *103*, 4413–4420.
- (41) Hubin, P. O.; Laurent, A. D.; Vercauteren, D. P.; Jacquemin, D. *Phys. Chem. Chem. Phys.* **2014**, *16*, 25288–25295.
- (42) Isaks, M.; Yates, K.; Kalanderopoulos, P. *J. Am. Chem. Soc.* **1984**, *106*, 2728–2730.
- (43) Kalanderopoulos, P.; Yates, K. *J. Am. Chem. Soc.* **1986**, *108*, 6290–6295.
- (44) Fischer, M.; Wan, P. *J. Am. Chem. Soc.* **1999**, *121*, 4555–4562.
- (45) Lukeman, M.; Wan, P. *J. Am. Chem. Soc.* **2002**, *124*, 9458–9464.
- (46) Flegel, M.; Lukeman, M.; Huck, L.; Wan, P. *J. Am. Chem. Soc.* **2004**, *126*, 7890–7897.
- (47) Lukeman, M.; Wan, P. *J. Am. Chem. Soc.* **2003**, *125*, 1164–1165.
- (48) Basaric, N.; Wan, P. *J. Org. Chem.* **2006**, *71*, 2677–2686.
- (49) Adamo, C.; Barone, V. *J. Chem. Phys.* **1999**, *110*, 6158–6170.
- (50) Rao, L.; Ke, H.; Fu, G.; Xu, X.; Yan, Y. *J. Chem. Theory Comput.* **2009**, *5*, 86–96.
- (51) Santra, B.; Michaelides, A.; Scheffer, M. *J. Chem. Phys.* **2007**, *127*, 184104.
- (52) Bousquet, D.; Fukuda, R.; Jacquemin, D.; Ciofini, I.; Adamo, C.; Ehara, M. *J. Chem. Theory Comput.* **2014**, *10*, 3969–3979.
- (53) Jacquemin, D.; Perpète, E. A.; Scuseria, G. E.; Ciofini, I.; Adamo, C. *J. Chem. Theory Comput.* **2008**, *4*, 123–135.
- (54) Krishnan, R.; Binkley, J. S.; Seeger, R.; Pople, J. A. *J. Chem. Phys.* **1980**, *72*, 650–654.
- (55) Cancès, E.; Mennucci, B.; Tomasi, J. *J. Chem. Phys.* **1997**, *107*, 3032–3041.
- (56) Scalmani, G.; Frisch, M. J.; Mennucci, B.; Tomasi, J.; Cammi, R.; Barone, V. *J. Chem. Phys.* **2006**, *124*, 094107.

- (57) Impropa, R.; Barone, V.; Scalmani, G.; Frisch, M. J. *J. Chem. Phys.* **2006**, *125*, 054103.
- (58) Frisch, M. J.; Trucks, G. W.; Schlegel, H. B.; Scuseria, G. E.; Robb, M. A.; Cheeseman, J. R.; Scalmani, G.; Barone, V.; Mennucci, B.; Petersson, G. A.; Nakatsuji, H.; Caricato, M.; Li, X.; Hratchian, H. P.; Izmaylov, A. F.; Bloino, J.; Zheng, G.; Sonnenberg, J. L.; Hada, M.; Ehara, M.; Toyota, K.; Fukuda, R.; Hasegawa, J.; Ishida, M.; Nakajima, T.; Honda, Y.; Kitao, O.; Nakai, H.; Vreven, T.; Montgomery, J. A., Jr.; Peralta, J. E.; Ogliaro, F.; Bearpark, M.; Heyd, J. J.; Brothers, E.; Kudin, K. N.; Staroverov, V. N.; Kobayashi, R.; Normand, J.; Raghavachari, K.; Rendell, A.; Burant, J. C.; Iyengar, S. S.; Tomasi, J.; Cossi, M.; Rega, N.; Millam, M. J.; Klene, M.; Knox, J. E.; Cross, J. B.; Bakken, V.; Adamo, C.; Jaramillo, J.; Gomperts, R.; Stratmann, R. E.; Yazyev, O.; Austin, A. J.; Cammi, R.; Pomelli, C.; Ochterski, J. W.; Martin, R. L.; Morokuma, K.; Zakrzewski, V. G.; Voth, G. A.; Salvador, P.; Dannenberg, J. J.; Dapprich, S.; Daniels, A. D.; Farkas, Ö.; Foresman, J. B.; Ortiz, J. V.; Cioslowski, J.; Fox, D. J. *Gaussian 09*, revision A.01; Gaussian, Inc.: Wallingford, CT, 2009.
- (59) Bader, R. F. W. *Chem. Rev.* **1991**, *91*, 893–928.
- (60) Bader, R. F. W. *Atoms in Molecules: A Quantum Theory*; International Series of Monographs on Chemistry 22; Oxford University Press: Oxford, U.K., 1990.
- (61) Keith, T. A. *AIMAll*, version 13.11.04; TK Gristmill Software: Overland Park, KS, 2014.
- (62) Brenlla, A.; Veiga, M.; Pérez Lustres, J. L.; Ríos Rodríguez, M. C.; Rodríguez-Prieto, F.; Mosquera, M. *J. Phys. Chem. B* **2013**, *117*, 884–896.
- (63) Grzegorzczek, J.; Filarowski, A.; Mielke, Z. *Phys. Chem. Chem. Phys.* **2011**, *13*, 16596–16605.
- (64) Ríos Rodríguez, S.; Ríos Rodríguez, M. C.; Mosquera, M.; Rodríguez-Prieto, F. *J. Phys. Chem. A* **2008**, *112*, 376–387.
- (65) Strandjord, A. J. G.; Smith, D. E.; Barbara, P. F. *J. Phys. Chem.* **1985**, *89*, 2362–2366.
- (66) Stasyuk, A. J.; Banasiewicz, M.; Cyranski, M. K.; Gryko, D. T. *J. Org. Chem.* **2012**, *77*, 5552–5558.
- (67) Wirz, J. *Pure Appl. Chem.* **1998**, *70*, 2221–2232.
- (68) Martinez, M. L.; Cooper, W. C.; Chou, P.-T. *Chem. Phys. Lett.* **1992**, *193*, 151–154.
- (69) Chen, K.-Y.; Hsieh, C.-C.; Cheng, Y.-M.; Lai, C.-H.; Chou, P.-T. *Chem. Commun.* **2006**, 4395–4397.
- (70) Piechowska, J.; Gryko, D. T. *J. Org. Chem.* **2011**, *76*, 10220–10228.
- (71) Matthews, W. S.; Bares, J. E.; Bartmess, J. E.; Bordwell, F. G.; Cornforth, F. J.; Drucker, G. E.; Margolin, Z.; McCallum, R. J.; McCollum, G. J.; Vanier, N. R. *J. Am. Chem. Soc.* **1975**, *97*, 7006–7014.
- (72) Bordwell, F. G.; Fried, H. E. *J. Org. Chem.* **1981**, *46*, 4327–4331.
- (73) Chen, J.; McAllister, M. A.; Lee, J. K.; Houk, K. N. *J. Org. Chem.* **1998**, *63*, 4611–4619.
- (74) Gilli, P.; Pretto, L.; Bertolasi, V.; Gilli, G. *Acc. Chem. Res.* **2009**, *42*, 33–44.
- (75) Mata, I.; Alkorta, I.; Molins, E.; Espinosa, E. *Chem.—Eur. J.* **2010**, *16*, 2442–2452.
- (76) Jablonski, M.; Solà, M. *J. Phys. Chem. A* **2010**, *114*, 10253–10260.
- (77) Poater, J.; Fradera, X.; Solà, M.; Duran, M.; Simon, M. *Chem. Phys. Lett.* **2003**, *369*, 248–255.
- (78) Espinosa, E.; Molins, E.; Lecomte, C. *Chem. Phys. Lett.* **1998**, *285*, 170–173.
- (79) Yanai, T.; Tew, D.; Handy, N. *Chem. Phys. Lett.* **2004**, *393*, 51–57.
- (80) Hammond, G. S. *J. Am. Chem. Soc.* **1955**, *77*, 334–338.
- (81) Barone, V.; Cossi, M. *J. Phys. Chem. A* **1998**, *102*, 1995–2001.
- (82) Cossi, M.; Rega, N.; Scalmani, G.; Barone, V. *J. Comput. Chem.* **2003**, *24*, 669–681.
- (83) Klamt, A.; Schüürmann, G. *J. Chem. Soc., Perkin Trans. 2* **1993**, 799–805.
- (84) Kirkwood, J. G. *J. Chem. Phys.* **1936**, *2*, 351–361.
- (85) Mills, S. G.; Beak, P. *J. Org. Chem.* **1985**, *50*, 1216–1224.
- (86) Emsley, J.; Freeman, N. *J. Mol. Struct.* **1987**, *161*, 193–204.
- (87) Powlings, J.; Bernstein, H. *J. Am. Chem. Soc.* **1951**, *73*, 4353–4356.